

Measurements of Photon Beam Flattening Filter Using an Anisotropic Analytical Algorithm and Electron Beam Employing Electron Monte Carlo

Mohammed El Adnani Krabch^{1,2}, Abdelouahed Chetaine³, Kamal Saidi^{2,3}, Fatima Zohra Erradi³, Abdelati Nourreddine^{3*}, Yassine Benkhouya³, Redouane El Baydaoui⁴,

1. Physics Department, Faculty of Sciences, Mohamed V University, Rabat, Morocco;
2. Department of Radiotherapy, Sheikh Khalifa Ibn Zaid Hospital, Casablanca, Morocco
3. Physics Department, Faculty of Sciences, Mohamed V University, Rabat, Morocco
4. Laboratory of Research in Health Sciences and Technologies, Hassan 1st University, Higher Institute of Health Sciences, Settat, Morocco

ARTICLE INFO

Article type:
Original Article

Article history:
Received: May30, 2018
Accepted: Oct 20, 2018

Keywords:
Linear accelerator
Algorithm
Monte Carlo Method
Radiotherapy

ABSTRACT

Introduction: This study aimed to report the measurement of photon and electron beams to configure the Analytical Anisotropic Algorithm and Electron Monte Carlo used in clinical treatment.

Material and Methods: All measurements were performed in a large water phantom using a 3-dimensional scanning system (PTW, Germany). For photon beams, the data were measured with a 0.125cc cylindrical chamber. For electron, the data were performed with a Roos chamber.

Results: In photon beams, flatness and symmetry for reference field size 10×10cm² were within the tolerance intervals. Flatness were 0.79% and 1.55% for X6MV and X18MV, respectively. Symmetry were 0.57 and 0.25 for X6MV and X18MV, respectively. The output factor vary between 0.83 and 1.11 for X6MV. Moreover, it varies between 0.74 and 1.09 for X18MV. The leaf transmission factors were 0.97% for X6MV and 1.14% for X18MV. The DLG were 1.31 and 1.34 for X6MV and X18MV, respectively. For electron beams, the quality index R₅₀ for applicator 15×15cm² were in the tolerance. Maximum depth dose for 6, 9, 12, 16 and 20MeV were 1.2, 1.9, 2.7, 2.99 and 2.4cm, respectively. Bremsstrahlung tail were 6MeV–2.86cm, 9MeV–4.32cm, 12MeV–5.96cm, 16MeV–7.93cm, and 20MeV–10.08cm per energy levels.

Conclusion: The obtained results and international recommendations were in a good agreement.

► Please cite this article as:

Krabch M El A, Chetaine A, Saidi K, Erradi FZ, Nourreddine A, Benkhouya Y, Baydaoui R El. Measurements of Photon Beam Flattening Filter Using an Anisotropic Analytical Algorithm and Electron Beam Employing Electron Monte Carlo. Iran J Med Phys 2019; 16: 200-209. 10.22038/ijmp.2018.31544.1372.

Introduction

A linear accelerator is a system that uses electromagnetic waves of high frequencies (close to 3000 MHz) to accelerate electrons up to very high energies (of the order of 25 MeV) through a linear tube. After passing through lead scatters, the produced electron beams can be used to treat superficial lesions, or to strike a metal target (tungsten), or to produce X-rays that can treat deeper tumors.

At Sheikh Khalifa Ibn Zaid Hospital in Casablanca, Morocco, a new linear accelerator Clinac iX S/N 5753 (Varian Medical System, USA) was recently installed with 2 photon beams of 6 and 18 MV energies and 5 electron beams of 6, 9, 12, 16, 20 MeV energies. After the installation of the machine, the medical physicist in the presence of the specialists from the manufacturing company must took several tests to verify the machine and the technical specification, if they corresponded to the clinical need. This step was called acceptance of the machine. The acceptance of

the machine was obligatory step, which served the purpose of checking the safety of radiation and controlling the mechanical and dosimetric parameters of the machine.

Once the acceptance tests were completed, the medical physicists performed the commissioning beam data measurements. The Varian had the upgraded version of Eclipse dosimetry software, in particular by making new algorithms available (Analytical Anisotropic Algorithm [AAA] and Electron Monte Carlo [eMC]). This calculation software allowed physicists to perform the ballistics treatment calculating the dose deposited by beams after contouring targets and organs at risk by physician. This made irradiation to the tumor as well as maintenance of the organs at risk and healthy tissues at its best.

The AAA calculation algorithm was developed by Dr. Waldemar Ulmer [1, 2] and Dr. Wolfgang Kaissl [3]. This algorithm uses a Monte Carlo model, the

*Corresponding Author: Tel: +212600113250; Email: krabch.adnani@gmail.com

integral components of the modeled beam are the main source of photons, the secondary source of photons (scattered), and the source of electron contamination.

The eMC algorithm is a clinically-used algorithm that calculates the dose distribution for high energy electron beams in a fast way [4]. This algorithm uses precalculations of particle transport in spheres with different diameters and constant density, meaning that it combines two components:

- A coupled multisource model of spatial phase for the simulation of electron and photon transport through the radiation of a linear accelerator
- The dose calculation code for the transport of electrons and photons.

The current study is a report of the performed measurements and the obtained results from the commissioning of this algorithm for clinical use. This study is conducted to assist medical physicists to perform commissioning of a new linear accelerator, provide the necessary information about equipment and the measurement conditions, and check the measured data before the first use of the machine for cancer treatment.

In order to configure AAA [5-8], there is a need to measure the percentage depth dose (PDD) curves, profiles crossplane, transmission factor, and dosimetric leaf gap (DLG). Fore MC algorithm [9-11], the PDD measurements for five applicators, PDD without applicator, and the profile in air were performed. All these measurements were performed in a large water phantom using a 3-dimensional scanning system MP3 water Phantom (PTW, Freiburg, Germany), with MEPHYSTO mc² software using a cylindrical chamber Semiflex 0.125cc and pinpoint 0.016cc for photon beams, plane parallel chamber with a sensitive volume 0.35cc for electron beams.

Materials and Methods

Clinac linear accelerator

In this article, all data and measurements were made using a medical accelerator called Clinac iX with multileaf collimator 120MLC. This accelerator has been installed at Sheikh Khalifa Ibn Zaid Hospital in Morocco since 2015. It can deliver dual energy of 6 MV and 18 MV photon beams with a maximum dose rate of 600 Gy/min, as well as multi-energy electron beams of 6, 9, 12, 16, and 20 MeV. The maximum treatment field size is 40×40 cm² that can be defined by a pair of X and Y jaws. It represents an evolution of the previous series of linacs, where it contains new treatment modalities like Volumetric Modulated Arc Therapy, as well as advances in imaging modalities. It is equipped with Portal Vision aS1000 MV Imaging System that allows the verification of the patient setups. This imaging system has an amorphous silicon detector with an active imaging area of 40×30 cm² (resolution of 1024×768). Another system is located at the gantry called the On-

Board Imager, this tool captures high-quality kV images in the treatment room for target localization, patient positioning, and motion management.

Multileaf collimator MLC

The Millennium 120-leaf MLC is a system that conforms to tumor volumes, to preserve healthy tissue and organs at risk. It consists of 120 leaves (a pair of 60 opposed leaves). These leaves can be used in the following 3 modes:

- Static mode reserved for the 3-dimensional conformal radiotherapy technique in which the leaves remain at a fixed position during treatment.
- Dynamic mode reserved for the intensity modulated conformal radiotherapy technique in which the leaves change the position during the treatment in order to modulate the intensity of the beam.
- Conformal arc mode in which the leaves always conform to the outer boundary of the target as the gantry rotates around the patient.

In order to include the effect of MLCs on dose calculation, Eclipse treatment planning systems requires two parameters, including transmission factor and DLG.

Commissioning beam data of the treatment planning system

The dosimetric data required for routine accelerator operation were performed according to the recommendations of The American Association of Physicists in medicine Task Group 106 (AAPM TG-106) and European Society for Radiotherapy and Oncology (ESTRO) codes of practice [12, 13] using an MP3 water phantom connected to a computer. The system is controlled for the acquisition of measurement data by MEPHYSTO mc² software.

Commissioning Photon Beams

The PDDs, profiles crossplane, transmission factor, and DLG were measured with a 0.125 cc cylindrical chamber; model 31010 Semiflex (PTW, Germany) for both ionization field and reference. The properties of the chamber includes an active length of 6.5mm and an internal diameter of 5.5mm. The output factor was measured with a PTW pinpoint chamber; model 31016 (PTW, Germany) with the nominal sensitive volume of 0.016 cc, the active length of 2.9mm, and internal diameter of 2.9mm.

Commissioning Electron Beams

The PDD measurements for each applicator, PDD without applicator, and the profile in air for a large field size 40×40 cm² were performed with a Roos plane parallel chamber; model 34001 (PTW, Germany) that has a radius of 7.8 mm and nominal sensitive volume of 0.35cc.

PDD and Profiles

The PDD is defined as the variation of dose absorbed in water $D_w(x, y) (z)$, on the axis of the beam

as a function of the depth of the measuring point for a constant SSD. For a given field size (f), it is generally normalized by the maximum value of the dose $Dw(x, y)$ (Z_{max}) on the axis of the beam multiplied by 100.

$$PDD(z) = \frac{D^f_{w(z,r\perp=0)}}{D^f_{w(z=z_{max},r\perp=0)}} * 100 \quad (1)$$

The PDD in a water environment depends on three parameters, including beam energy, irradiation field size, and source-surface distance. For photon beams, PDD was measured for a variety of square fields with the size ranged from $4 \times 4 \text{ cm}^2$ to $40 \times 40 \text{ cm}^2$ at the nominal treatment distance $SSD=100\text{cm}$. The ratio of ionizations J20 and J10 were at 20 cm and 10 cm depths, respectively, for reference field size $10 \times 10 \text{ cm}^2$ called quality index. This factor gives an idea of the photon beam stability. For electron beams, PDD was measured for each applicator and without applicator for a large field size $40 \times 40 \text{ cm}^2$ at $SSD=100\text{cm}$. The quality index is the depth of half-attenuation in water, R_{50} for field size of $15 \times 15 \text{ cm}^2$.

The dose profile corresponds to the variation of the dose in water, along with an axis perpendicular to the beam axis, at a different depth and for a different field size. Dose values are generally normalized by the value of the dose at beam axis.

$$PRD(z) = \frac{D^f_{w(z,r\perp)}}{D^f_{w(z,r\perp=0)}} \quad (2)$$

This equation is used to determine the dose rate outside the beam axis at any depth in the water from the reference dose rate, the collimating aperture factor, and the PDD. An area called "penumbra" is corresponding to the area where the dose at the edge of the field is between 20% and 80% of the dose on the axis.

Photon beam profiles were measured in principal X and Y axes at $SSD=100\text{cm}$, at 5 depth (Z_{max} , 5, 10, 20, and 30 cm) in water, for a variety of square fields with the size within the range of 4×4 - $20 \times 20 \text{ cm}^2$. The water phantom cannot measure complete profiles for field sizes exceeding 20 cm, where the treatment planning system TPS accepts half profiles. In the current study, we cannot expose the data to these fields. Electron beam profile without applicator in air was measured for a large field size of $40 \times 40 \text{ cm}^2$ at $SSD=95\text{cm}$.

For beam profiles analysis, field size was defined at 50% beam profile intensity. Field symmetry was defined as the maximum ratio between symmetric points within the flattened region (80% of the field size) expressed in percentage.

$$S = \frac{D(x)}{D(-x)} * 100 \quad (3)$$

Homogeneity was defined within the flattened region as:

$$H = \frac{D_{max}-D_{min}}{D_{max}+D_{min}} * 100 \quad (4)$$

Output factor

The output factor (OF) is defined by the ratio of the absorbed dose in water $Dw(x, y)$, on the beam axis, for a field size (X, Y), and the dose absorbed in water $Dw(10, 10)$ at the same distance and same depth, for the reference field size (10, 10) [14].

$$OF(x, y) = \frac{Dw(x,y)}{Dw(10,10)} \quad (5)$$

This factor makes it possible to take into account the variation of the scatter in the head of the accelerator and in water phantom, which allows to calculate the dose rate on the beam axis for any field size from the reference dose rate.

In this study, output factors for photon beams were measured at 5cm ($SSD=95\text{cm}$) and 10cm ($SSD=90\text{cm}$) depth respectively for X6MV and X18MV, for squared and rectangular fields in water with the same range as PDDs and profiles.

Transmission factor

The multileaf collimator do not completely block radiation as a small part, which is transmitted directly among the leafs[15]. The Transmission factor can be estimated as the ratio of measured dose, in an open field, and the dose measured using the same size for all MLCs closed behind the jaws.

$$TF = \frac{R_{closed}}{R_{open}} \quad (6)$$

Dosimetric leaf gap (DLG)

A part of radiation could pass through the opposite leaves even though they are completely closed, because the Varian MLCs are characterized by a rounded leaf tips. Therefore, DLG as an important factor must be measured to quantify the contribution of this transmission to the calculation of the dose delivered to the patient. In fact, DLG is related to the space between the light field and the irradiation field formed by the MLCs [15-17].

To calculate DLG factor, the reading transmission values for banks A (RT, A) and B (RT, B) are measured, and averaged.

$$RT = \frac{RT,A+RT,B}{2} \quad (7)$$

Afterwards, the readings (R_g) for the eight moving gaps (2, 4, 6, 8, 10, 14, 16, and 20mm) are taken, since the transmission through the MLC contributes to the gap readings.

$$R_g T = RT (1 - g/120) \quad (8)$$

The corrected gap reading R_g' is calculated for each gap g . $R_g' = R_g - R_g T$ (9)

A linear function $g(R_g') = aR_g' + b$ is fitted, the DLG is defined as the extrapolated gap that would give zero corrected reading at zero gap, DLG equal the absolute value of b .

Results

Photon Beams

a) PDD

The PDD curves of all photon energies increasing the area of field size affect the dose value in tail region due to the contribution amount of particle (figures 1 and 2). The measured maximum depth dose (d_{max}), quality indices of both photon beams for field size of $10 \times 10 \text{ cm}^2$ (Table 1) were used for characterizing the photon beams energy.

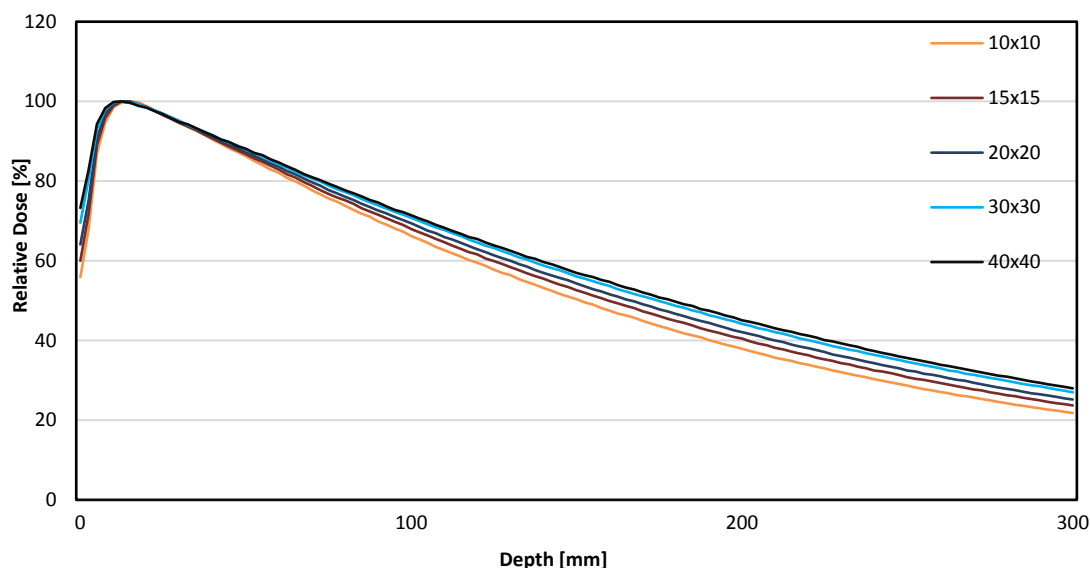


Figure 1. Percentage depth dose graph using 6 MV for field sizes

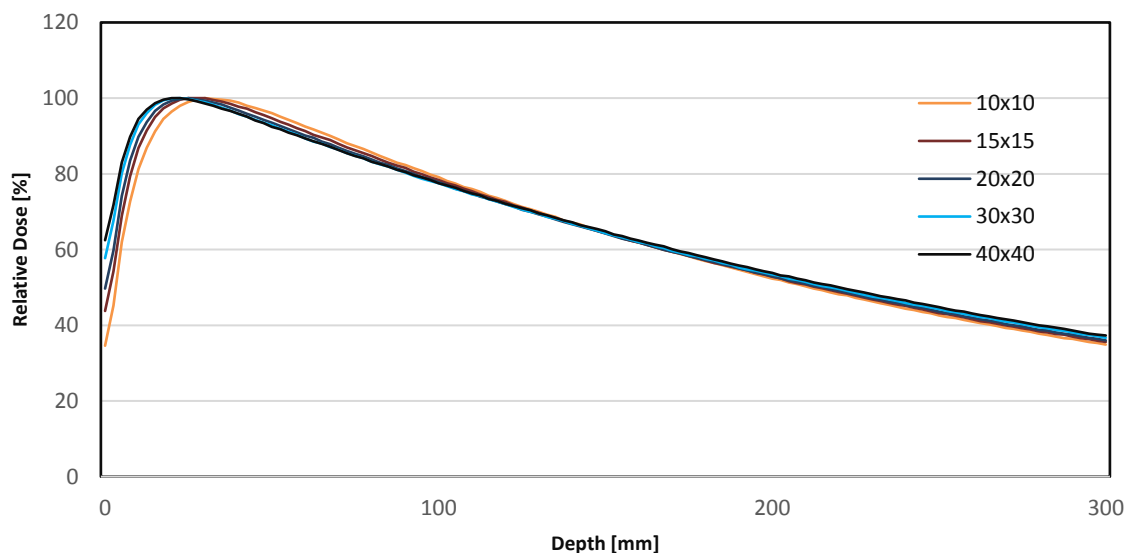


Figure 2. Percentage depth dose graph using 18 MV for field sizes

Table 1. Depth dose parameter using 6 MV and 18 MV energies for different field sizes

Energy	Field Size	D _{max} (cm)	PDD(10cm)	PDD(20cm)	TPR (20,10)
X6 MV	10×10 cm ²	1.50	66.23	37.93	0.6657
X18 MV	10×10 cm ²	3.00	79.07	52.34	0.7785

b) Profiles

Figures 3 and 4 show the profile curves of some photon energies, the half profiles were presented in figure 5. The data extracted from curves (Table 2) show that the flatness rates were 0.79% and 1.55% for X6MV and X18MV, respectively. Moreover, symmetry values were 0.57% and 0.25% for X6MV and X18MV, respectively.

For X6MV the left and right penumbra region were 5.78 ± 0.40 mm and 5.61 ± 0.37 mm, respectively. Additionally, with regard to X18MV, the penumbra was 7.93 ± 0.69 mm in left side and 7.31 ± 0.66 mm in right side.

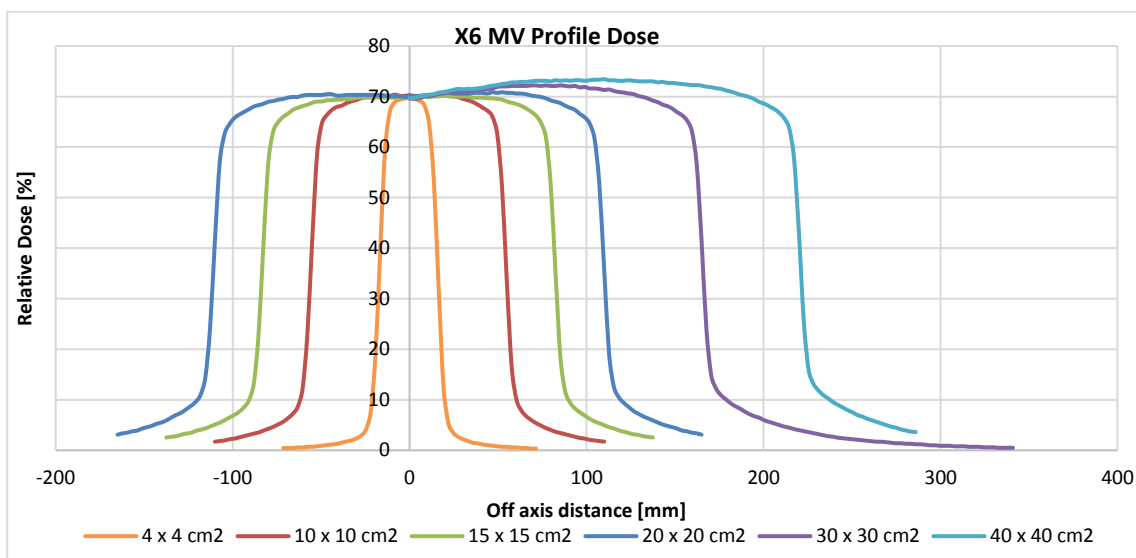


Figure 3. Profile dose graph using 6 MV photon energy for field sizes

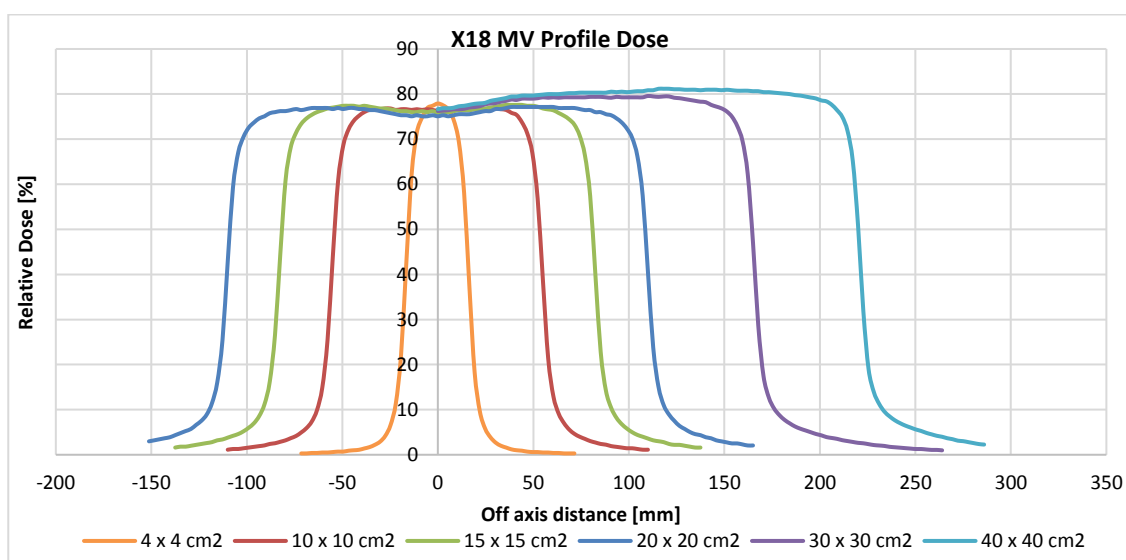


Figure 4. Profile dose graph using 18 MV photon energy for field sizes

Table 2. Profile dose parameters using 6 MV and 18 MV energies for different field sizes

Energy	Field Size(cm ²)	Flatness (%)	Symmetry (%)	Left Penumbra (mm)	Right Penumbra (mm)
X6 MV	3×3	8.91	2.01	5.39	5.27
	4×4	5.69	0.89	5.46	5.24
	6×6	2.15	0.52	5.64	5.44
	8×8	1.30	0.38	5.82	5.63
	10×10	0.79	0.57	5.96	5.66
	12×12	0.66	0.51	5.98	5.73
	15×15	1.06	0.78	6.09	5.90
X18 MV	20×20	1.64	0.88	6.18	5.98
	3×3	1.33	0.77	6.70	6.65
	4×4	8.06	0.80	6.94	6.96
	6×6	4.34	0.61	7.29	7.27
	8×8	2.21	0.43	7.34	7.42
	10×10	1.55	0.25	7.47	7.64
	12×12	1.39	0.48	7.56	7.78
15×15	1.26	0.64	7.78	7.86	
20×20	1.65	0.70	8.08	7.97	

e) Output factor

Figure 6 illustrates the output factor curves for X6 MV and X18 MV. Considering X6 MV, this factor varied between 0.83 for the smaller field size 4×4 cm² and 1.11 for the larger field size 40×40 cm². Regarding X18 MV, it varies between 0.74 and 1.09 for field size 4×4 cm² and 40×40 cm², respectively.

d) Transmission factor

Table 3 summarizes the measurement and the mean value of MLC transmission factor for the Bank A and Bank B.

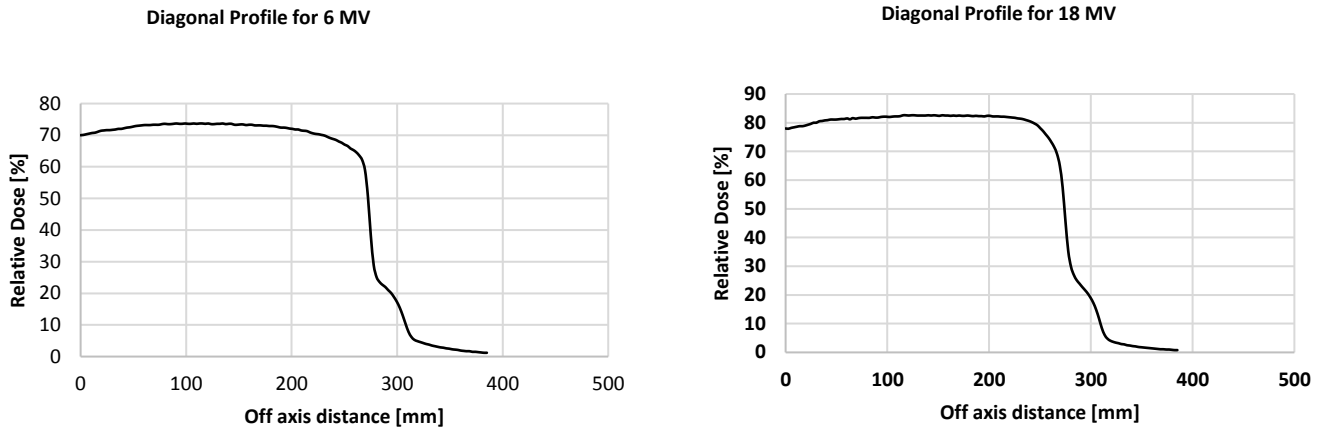


Figure 5. Diagonal profile graph for field size 40x40 cm² using different energies 6 MV & 18 MV

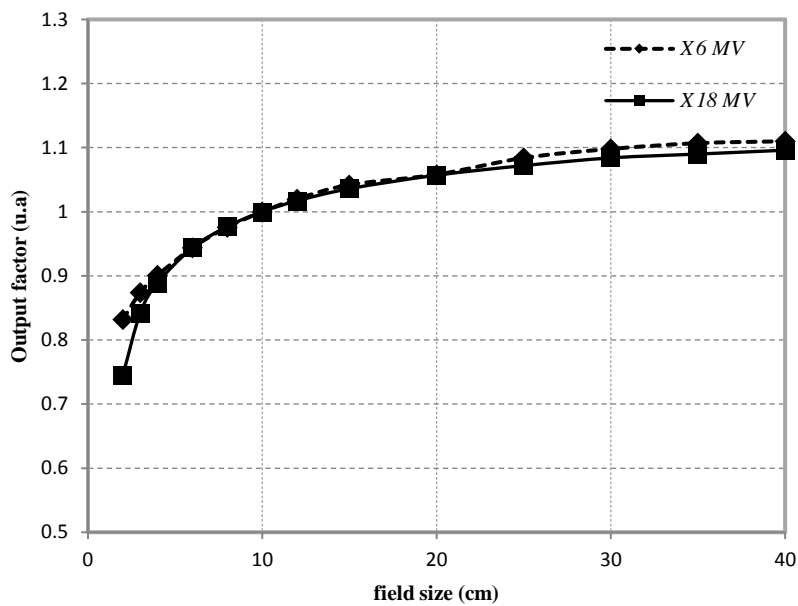


Figure 6. Output factor for different field sizes and energies

Table 3. Transmission factor for X16 MV and X18 MV

Energy	Reading average « MLC closed »	Reading average « MLC opened »	Transmission Factor
X6 MeV	0.009	0.93	0.009677419
X18 MeV	0.01	0.877	0.011402509

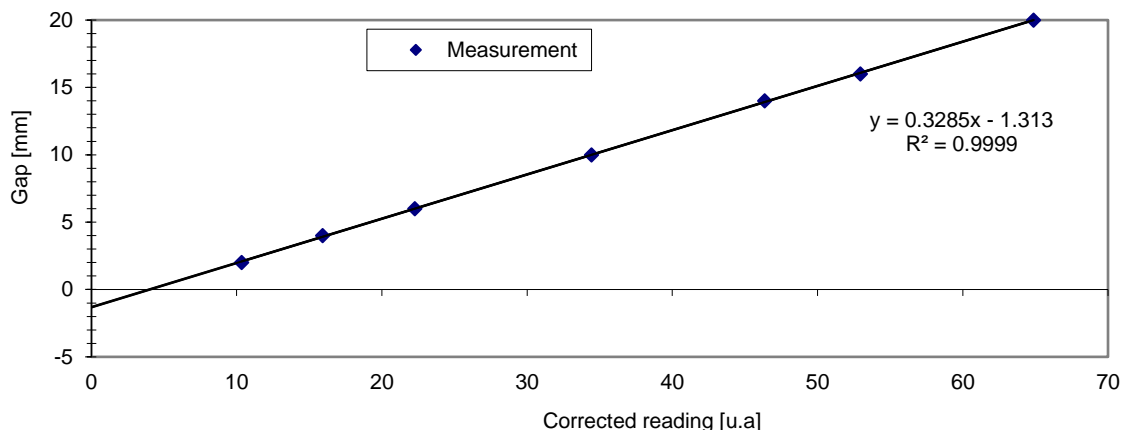


Figure 7. Obtained results from DLG measurements for X6MV

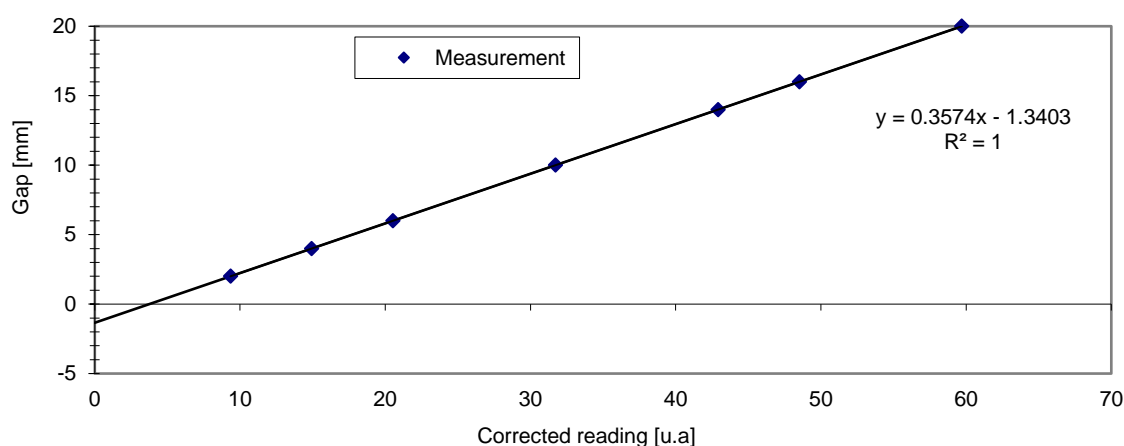


Figure 8. Obtained results from DLG measurements for X18MV

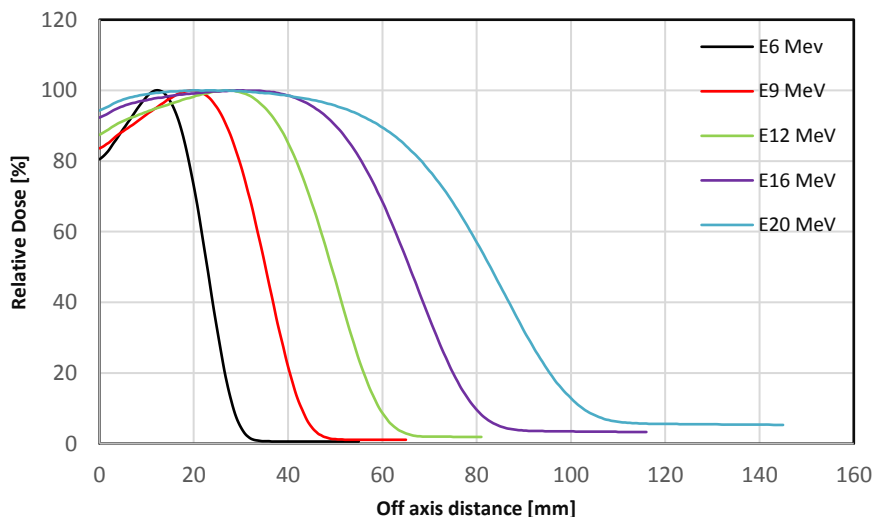


Figure 9. Percentage depth dose graph for applicator 15x15 cm² using different energies

e) DLG Measurement

The figure 7 and 8 show the dosimetry leaf gap curves for all photon beams, and the DLG value correspond to zero corrected reading.

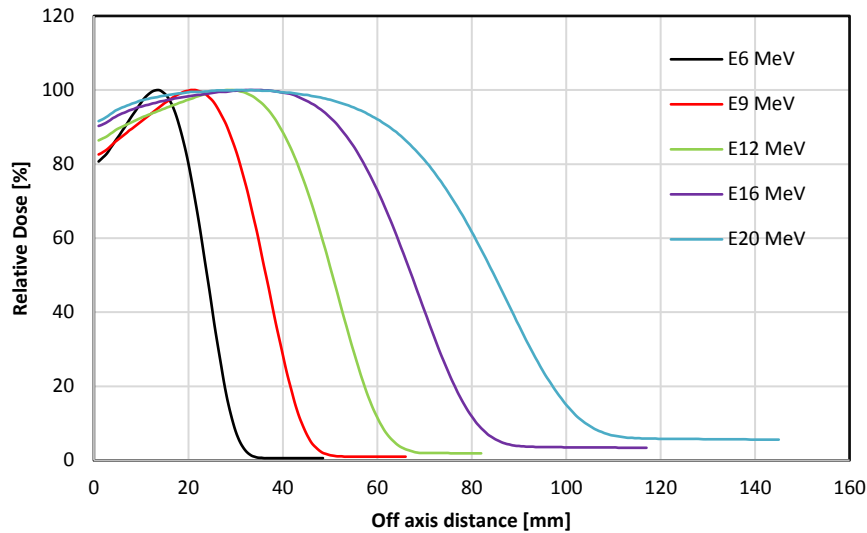


Figure 10. Percentage depth dose graph for field size 40x40 cm2 without applicator using different energies

Table 4. Depth dose parameter using 6 MV and 18 MV energies for different field sizes

Energy	Applicator	Dmax(mm)	R50 (mm)	R90 (mm)	RP (mm)
E6 MeV	6x6	12.01	22.95	16.79	28.27
	10x10	12.49	22.80	17.05	28.56
	15x15	12.49	22.85	17.11	28.63
	20x20	12.03	22.86	17.07	28.63
	25x25	12.49	22.90	17.11	28.74
	40x40*	12.49	22.97	17.15	28.82
E9 MeV	6x6	18.99	34.88	26.53	42.86
	10x10	19.50	35.14	26.86	43.16
	15x15	19.52	35.20	26.93	43.25
	20x20	19.97	35.26	26.98	43.33
	25x25	19.51	35.32	27.01	43.40
	40x40*	20.00	35.43	27.22	43.33
E12 MeV	6x6	24.47	48.60	36.72	59.44
	10x10	27.01	49.09	37.86	59.53
	15x15	27.01	49.21	37.99	59.66
	20x20	27.00	49.21	37.86	59.79
	25x25	26.98	49.32	38.03	59.84
	40x40*	27.52	49.49	38.38	59.88
E16 MeV	6x6	25.50	64.03	46.03	79.41
	10x10	29.50	65.60	49.82	79.31
	15x15	29.99	65.74	50.08	79.34
	20x20	28.51	65.77	49.89	79.42
	25x25	31.00	65.93	50.13	79.48
	40x40*	33.48	66.26	50.93	79.72
E20 MeV	6x6	18.00	78.93	52.03	100.50
	10x10	19.96	82.49	58.03	100.57
	15x15	23.99	82.91	59.44	100.78
	20x20	23.51	83.00	59.31	100.76
	25x25	21.99	83.19	59.69	100.88
	40x40*	29.99	83.76	61.59	101.01

Electron Beams

a) PDD

Figure 9 and 10 indicates PDD curves of all electron energies for reference applicator and for large field size 40 x 40 cm² without applicator respectively; moreover, table4 tabulates the data extracted from the curves. The quality index R₅₀ for applicator 15x15 cm²were within tolerance (R₅₀< 4 g.cm⁻² for E₀< 10 MeV and R₅₀>4 g.cm⁻² for E₀>10 MeV). The maximum depth dose for the energies of 6, 9, 12, 16, and 20 MeV were 1.2, 1.9,

2.7, 2.99, and 2.4 cm, respectively. Bremsstrahlung tail per energy levels were obtained as 6 MeV–2.86 cm, 9 MeV–4.32 cm, 12 MeV–5.96 cm, 16 MeV–7.93 cm and 20 MeV–10.08 cm.

b) Profile in air

Figure 11 demonstrates the data for electron beams. As can be seen, the profile in air for a large field size was40x40cm² for electron beams.

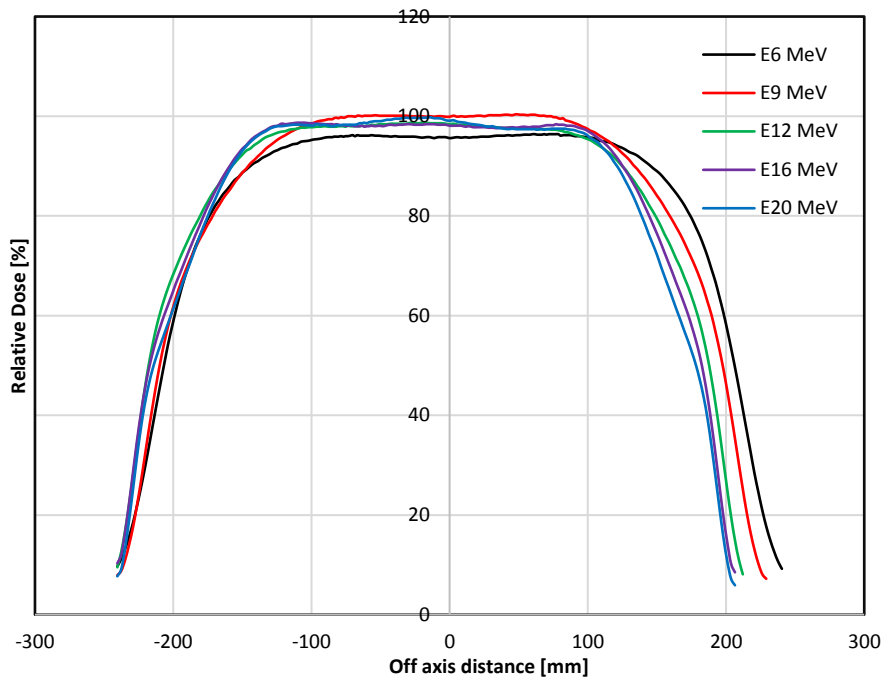


Figure 11. Profile in air graph for field size $40 \times 40 \text{ cm}^2$ without applicator using different energies

Discussion

Photon Beams

a) PDD

All the parameters were within the recommended values defined in IAEA TRS398 ($QI < 0.7$ for X6 MV, $QI > 0.7$ for X18 MV) [18], which are presented in Table 1. Energy stability is tested by ensuring that d_{max} (1.5cm and 3cm for X6MV and X18MV, respectively) and QI (0.6657 and 0.7785 for X6MV and X18MV, respectively) does not vary within the time for photon beam.

b) Profiles

Table 2 shows the data extracted from curves. Flatness and symmetry of both photon beams for reference field size $10 \times 10 \text{ cm}^2$ were within the tolerance intervals (flatness $< \pm 3\%$, Symmetry $< 2\%$). A small difference in doses was found between the left and right penumbra region, the penumbra value increased with the field size due to scattering within the water phantom and with the energy.

c) Output factor

As shown in figure 6, the output factor of photon beams increased when field size became greater due to more scattered components of radiation in bigger sizes.

d) Transmission factor

The MLC transmission factor were obtained as 0.97% and 1.14% for 6 MV and 18 MV, respectively. This factor can increase along with the energy since when energy increases more particle penetrates the leaves.

e) DLG Measurement

The DLG curves were linear with a correlation coefficient equal to 99.99% and 100% for photon energy X6 MV and X18 MV, respectively. After the extrapolation of the curves, the values of the DLG factors were 1.31 and 1.34 for X6 MV and X18 MV in order to have zero corrected reading, respectively.

Electron Beams

a) PDD

As illustrated in figures 9 and 10, the curve of the PDD of an electron beam is characterized by a high surface dose, followed by a rapid dose increase to d_{max} . Beyond d_{max} , there is a fast descent and the curve ends with a region of low dose, which is the tail of bremsstrahlung.

b) Profile in air

In this case, the profile is accepted without checking the values of the symmetry and flatness; therefore, the profile forms are verified.

Conclusion

The present study aimed to measure the commissioning of new delivery system of Clinac iX and employ it into the treatment planning system of Eclipse. In doing so, the dosimetric data were compared with a model given by Varian, which revealed good respect manufacturer margins and specifications.

Acknowledgment

We wish to thank all the staff of Sheikh Khalifa Ibn Zaid Hospital where the data acquisition was carried out for this study. In addition, we would like to express our sincere thanks to Mrs DINO Hanane

radiation technologue for her excellent support in this work.

References

1. Ulmer W, Harder D. A triple Gaussian pencil beam model for photon beam treatment planning. *Zeitschrift für medizinische Physik*. 1995 Jan 1;5(1):25-30.
2. Ulmer W, Harder D. Applications of a triple Gaussian pencil beam model for photon beam treatment planning. *Zeitschrift für Medizinische Physik*. 1996 Jan 1;6(2):68-74.
3. Ulmer W, Kaissl W. The inverse problem of a Gaussian convolution and its application to the finite size of the measurement chambers/detectors in photon and proton dosimetry. *Physics in Medicine & Biology*. 2003 Mar 5;48(6):707-27.
4. Neuenschwander H, Mackie TR, Reckwerdt PJ. MMC-a high-performance Monte Carlo code for electron beam treatment planning. *Physics in Medicine & Biology*. 1995 Apr;40(4):543-74.
5. Fogliata A, Nicolini G, Vanetti E, Clivio A, Cozzi L. Dosimetric validation of the anisotropic analytical algorithm for photon dose calculation: fundamental characterization in water. *Physics in Medicine & Biology*. 2006 Feb 21;51(6):1421-38.
6. Ulmer W, Pyyry J, Kaissl W. A 3D photon superposition/convolution algorithm and its foundation on results of Monte Carlo calculations. *Physics in Medicine & Biology*. 2005 Apr 6;50(8):1767-90.
7. Van Esch A, Tillikainen L, Pyykkonen J, Tenhunen M, Helminen H, Siljamäki S, et al. Testing of the analytical anisotropic algorithm for photon dose calculation. *Medical physics*. 2006 Nov;33(11):4130-48.
8. Sievinen J, Ulmer W, Kaissl W. AAA photon dose calculation model in Eclipse. Palo Alto (CA): Varian Medical Systems. 2005.
9. Arunkumar T, Varatharaj C, Ravikumar M, Sathiyam S, Shwetha B. Commissioning and validation of the electron Monte Carlo dose calculation at extended source to surface distance from a medical linear accelerator. *International Journal of Medical Research and Review*. 2016.
10. Yang X, Lasio G, Zhou J, Lin M, Yi B, Guerrero M. Commissioning of Electron Monte Carlo in Eclipse Treatment Planning System for TrueBeam. *Med. Phys.* 2014; 41:362-6.
11. Antolak JA, Bieda MS, Hogstrom KR. A Monte Carlo method for commissioning electron beams. In *The Use of Computers in Radiation Therapy*. Springer, Berlin, Heidelberg. 2000 ; 449-51.
12. Das IJ, Cheng CW, Watts RJ, Ahnesjö A, Gibbons J, Li XA, et al. Accelerator beam data commissioning equipment and procedures: report of the TG-106 of the Therapy Physics Committee of the AAPM. *Medical physics*. 2008 Sep 1;35(9):4186-215.
13. Aletti P, Bey P, Chauvel P, Chavaudra J, Costa A, Donnareix D, et al. Recommendations for a quality assurance programme in external radiotherapy. 1995;2.
14. Mayilvaganan A, Athiyaman H, Chougule A. Analysis of Accuracy of Interpolation Methods in Estimating the Output Factors for Square Fields in Medical Linear Accelerator. *Iranian Journal of Medical Physics*. 2017;14(2):75-86.
15. Varadharajan E, Ramasubramanian V. Commissioning and Acceptance Testing of the existing linear accelerator upgraded to volumetric modulated arc therapy. *Reports of Practical Oncology & Radiotherapy*. 2013 Sep 1;18(5):286-97.
16. Szpala S, Cao F, Kohli K. On using the dosimetric leaf gap to model the rounded leaf ends in VMAT/RapidArc plans. *Journal of applied clinical medical physics*. 2014 Mar 1;15(2):67-84.
17. Mullins J, DeBlois F, Syme A. Experimental characterization of the dosimetric leaf gap. *Biomedical Physics & Engineering Express*. 2016 Dec 16;2(6):065013.
18. IAEA. Absorbed Dose Determination in External Beam Radiotherapy. IAEA Technical Reports Series No. 398. 2000.